

$\text{Bi}_{3.9}\text{Sr}_{3.3}\text{Ca}_{1.3}(\text{Cu}_{0.961}\text{Fe}_{0.039})_3\text{O}_x$: A high- T_c structure close to the two-dimensional limit

B. vom Hedt, R. Noetzel, W. Lißbeck, H. Bach, and K. Westerholt

Lehrstuhl für Experimentalphysik/Festkörperphysik, Ruhr-Universität Bochum, D-44780 Bochum, Germany

B. Freitag

Physikalisches Institut, Universität zu Köln, D-50937 Köln, Germany

(Received 4 November 1994)

We report the synthesis of single crystals of $\text{Bi}_{3.9}\text{Sr}_{3.3}\text{Cu}_{1.3}(\text{Cu}_{0.961}\text{Fe}_{0.039})_3\text{O}_x$, which can be regarded as an intergrowth of one half of the $\text{Bi}_2\text{Sr}_2\text{CaCu}_2\text{O}_8$ and one half of the $\text{Bi}_2\text{Sr}_2\text{Cu}_3\text{O}_{10}$ unit cell and is stabilized by the substitution of Fe for Cu. The compound possesses the strongest two-dimensional character of the superconducting properties among the bulk high- T_c structures known until now. From the scaling behavior of the reversible magnetization we derive an anisotropy parameter $\gamma \approx 10^3$ for the ratio of the penetration depths λ_c/λ_{ab} . We observe a magnetic irreversibility line with a maximum irreversibility temperature about 10 K below T_c and a reentrance behavior at low fields.

The quasi-two-dimensional (2D) character of superconductivity is one of the most important features of the high- T_c superconductors and gives rise to interesting phenomena in the behavior of the vortex lattice, which are under intense discussion in the current literature.¹⁻³ Among the actual topics is a Kosterlitz-Thouless (KT) type of phase transition below T_{c0} (Ref. 4) and a vortex lattice melting with a crossover from 2D to 3D melting.^{5,6} A reentrance of the melting line in the 3D range at low magnetic fields has been predicted theoretically but has not yet been observed experimentally.¹

The degree of the anisotropy of a high- T_c structure expressed quantitatively in terms of the anisotropy ratio of the penetration depths $\gamma = \lambda_c/\lambda_{ab}$ is an essential parameter determining the properties of the vortex lattice. With increasing γ value thermal fluctuations below T_{c0} become increasingly important and a lowering of the vortex lattice melting temperature and the crossover field from 2D to 3D behavior is expected. Simultaneously anomalous contributions to the thermodynamic quantities develop which can change the properties of the superconductor within a certain transition width below T_{c0} dramatically compared to the London theory. A quantitative theory taking these thermal fluctuations into account is currently being developed.²

Detailed measurements on $\text{Bi}_2\text{Sr}_2\text{CaCu}_2\text{O}_8$ [Bi(2212)] single crystals representing the high- T_c phase with the strongest 2D character [anisotropy ratio $\gamma = 50-200$ (Refs. 6 and 7)] have contributed considerably to an understanding of the physics of the vortex lattice in the temperature range dominated by thermal fluctuations. But even in the Bi(2212) phase this interesting temperature interval below the mean-field transition temperature T_{c0} has a width of about 2 K only.^{3,5}

The main aim of this paper is the introduction of a structure from the Bi-Sr-Ca-Cu-O system that has an anisotropy ratio about one order of magnitude larger than Bi(2212). This phase exhibits a much broader anomalous range below T_{c0} with remarkable features which have not been observed in the other high- T_c compounds before.

The crystals for the present work were grown by a modified Bridgman-Stockbarger technique, as described in detail elsewhere.^{8,9} For the present crystal growing process we started with a melt of the composition 2.4:2:1:2 referring to the metallic components of Bi_2O_3 , SrO, CaO, and CuO and replaced 2 at. % of Cu by Fe_2O_3 . The resulting platelet-shaped single crystals had dimensions up to $3 \times 2 \times 0.1 \text{ mm}^3$, very similar to Bi(2212) single crystals. With a quantitative electron microprobe analysis of different crystals we determined a homogeneous composition $\text{Bi}_{3.9}\text{Sr}_{3.3}\text{Ca}_{1.3}(\text{Cu}_{0.961}\text{Fe}_{0.039})_3\text{O}_x$; this is definitely different from that determined for the Bi(2212) phase, for which we typically get $\text{Bi}_{2.03}\text{Sr}_{2.0}\text{Ca}_{0.9}\text{Cu}_{2.0}\text{O}_x$. An x-ray rocking curve of the (009) Bragg reflection (see the inset of Fig. 1) gave a width of the rocking curve of 0.5° , a value also comparable with that of good quality Bi(2212) crystals.

In Fig. 1 we show the (001) Bragg reflection spectra of a crystal for the new phase and a Bi(2212) single crystal in direct comparison. The reflections can be indexed as shown

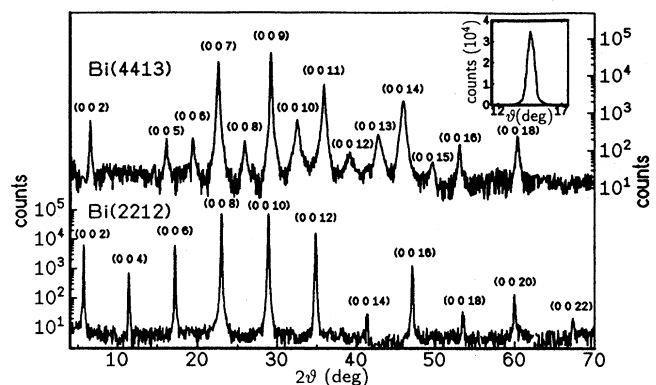


FIG. 1. (00 l) Bragg reflection pattern of a Bi(4413) crystal (upper panel) and a Bi(2212) crystal (lower panel). The peaks have been indexed with the c -axis lattice parameter $c = 27.6 \text{ \AA}$ and 30.6 \AA , respectively. The inset shows the rocking curve of the Bi(4413) (009) reflection.

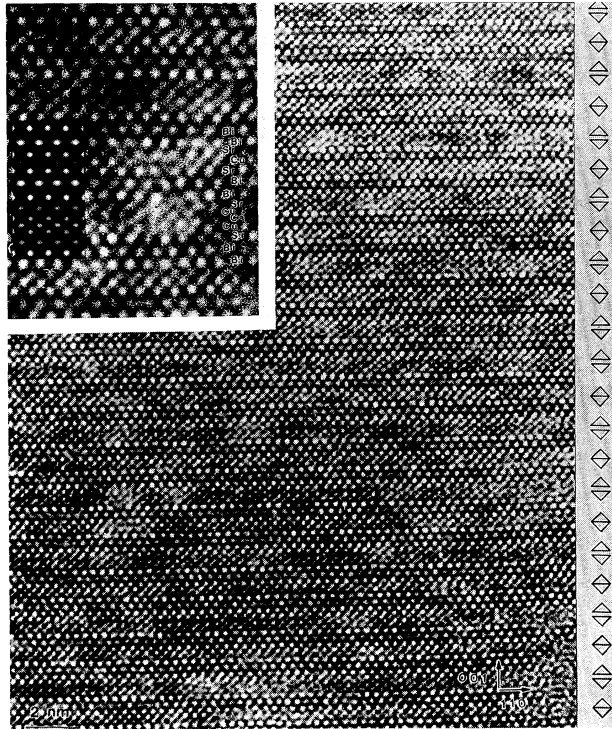


FIG. 2. HRTEM projection of Bi(4413) along the [110] direction. The inset shows an expanded view of the unit cell block compared to the image from a computer simulation. The symbols on the right margin denote the position of the CuO_2 layers.

in the figure with a c -axis lattice parameter of 27.6 and 30.6 Å. One should note that for the new phase (00 l) reflections with l even and l odd occur, whereas for the Bi(2212) phase the selection rules for the space group A_{2mm} only allow for reflections with l even. This shows that the symmetry of the new phase is lower.

In order to reveal the origin of the new periodicity along the c axis we used high-resolution lattice imaging technique (HRTEM) on a Philips CM30 transmission electron microscope with a Tracor Northern HPGc detector at 300 kV beam voltage. The lattice image in Fig. 2 projected along the [110] direction reveals that the new unit cell results from an intergrowth of one half of the Bi(2212) and one half of the Bi(2201) unit cell. Assuming the space group $Pmm2$ we got a reasonable agreement between the calculated and the measured intensities of the Bragg reflections in Fig. 1. In the systematics of the nomenclature of the Bi-based high- T_c series the new phase should be denoted by Bi(4413).¹⁰ The composition determined by the microprobe analysis (see above) is in reasonable agreement, if one regards that the Sr and Ca can interchange the positions and defects in the Sr/Ca lattice can occur, similar to the Bi(2212) phase.

In the HRTEM study we found that stacking faults are rather frequent in the new structure. The image in Fig. 2, e.g., shows one additional Bi(2212) block as a stacking fault. This stacking faults cause the slight line broadening of the Bragg reflections observed in Fig. 1.

Since the Bi(2201) phase has a maximum T_c of about 25 K, in the new Bi(4413) phase only the Bi(2212)-type CuO_2

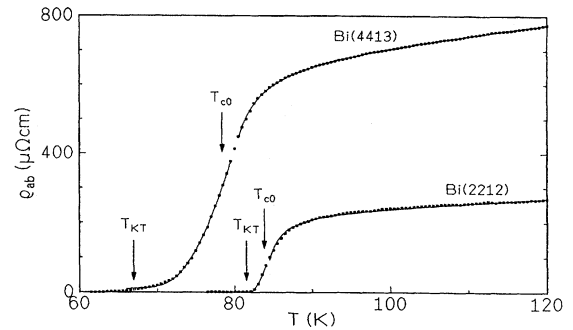


FIG. 3. Resistivity versus temperature for Bi(4413) and Bi(2212). The drawn lines are theoretical curves (see main text). T_{c0} and T_{KT} denote the mean-field transition temperature and the Kosterlitz-Thouless temperature, respectively.

double layers contribute to the superconductivity at high temperatures. Thus the distance between the superconducting layers increased by 12 Å compared to Bi(2212) and much more pronounced 2D behavior can be expected.

In Fig. 3 we show the (ab)-plane resistivity measured by a low-frequency ac technique on a Bi(4413) and a Bi(2212) crystal. The transition temperature of Bi(4413) is shifted towards lower temperatures by about 6 K and the transition is strongly broadened. We found that this broadening is a well reproducible and intrinsic phenomenon of the Bi(4413) single crystals and is caused by the strong 2D character and not by a chemical inhomogeneity. Comparable widths of the resistively measured superconducting transition have been observed on layered, epitaxially grown superlattices based on YBaCuO/PrBaCuO with nonsuperconducting PrBaCuO interlayers.¹¹

In Fig. 3 we show that $\rho(T)$ can be fitted perfectly by using the Aslamasov-Larkin formula for the excess conductivity above the mean-field transition temperature T_{c0} :¹² $\Delta\sigma = (e^2/16\hbar s)\tau^{-1}$ [$\tau = (T - T_{c0})/T_{c0}$ and s being the layer distance]. Below T_{c0} the classical Kosterlitz-Thouless formula for a 2D superconductor above the vortex-antivortex unbinding temperature T_{KT} :¹³ $\rho = a\rho_n \exp[-2(b\tau_c/\tau)^{1/2}]$ fits $\rho(T)$ very well [$\tau_c = (T_{c0} - T_{KT})/T_{KT}$, $\tau = (T - T_{KT})/T_{KT}$ and a, b constants of order unity]. From the fit in Fig. 3 we derive $T_{c0} = 78.5$ K and $T_{KT} = 67$ K for Bi(4413). The same analysis for Bi(2212) in Fig. 3 gave $T_{c0} = 85.5$ K and $T_{KT} = 83.2$ K. Thus the temperature interval with KT-type behavior increases by nearly one order of magnitude in Bi(4413) compared to Bi(2212), clearly indicating the strongly enhanced 2D character.

In Fig. 4 we show the low-field dc susceptibility of the Bi(4413) crystal. The susceptibility has been measured by a noncommercial superconducting quantum interference device magnetometer with the field direction along the c axis of the crystals.¹⁴ The reversible range of the susceptibility (see upper part of Fig. 4) marked by the deviation between the zero-field-cooled and the field-cooled susceptibility is extremely broad in Bi(4413), extending down to about 13 K below T_{c0} . For Bi(2212) the corresponding reversible width is only 2 K.

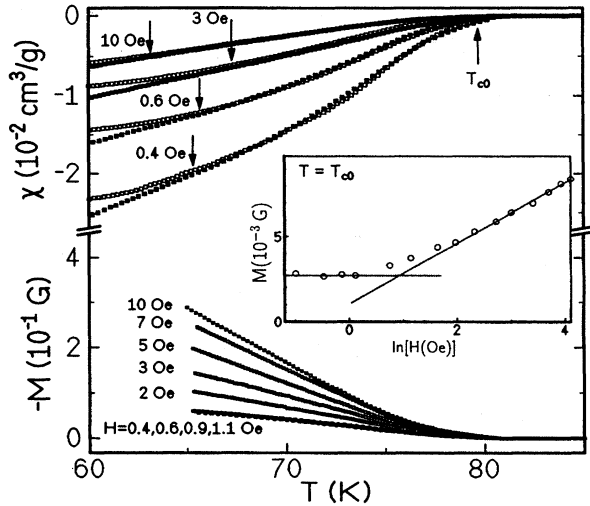


FIG. 4. Field-cooled and zero-field-cooled susceptibility versus temperature (empty and filled symbols) of Bi(4413) at different applied fields given in the figure (upper panel). The arrows indicate the irreversibility temperature. Reversible magnetization versus temperature (lower panel). The inset shows the field dependence of the magnetization at T_{c0} .

The reversible range observed in the susceptibility coincides with the temperature range with KT-type behavior in the resistivity in Fig. 4. This is an important further indication that anomalous thermal fluctuations and not a chemical inhomogeneity causes the broadening of $\rho(T)$ in Fig. 3.

We find that for applied magnetic fields below 1 Oe the reversible magnetization is field independent (Fig. 4), and for higher fields $M(T)$ increases logarithmically with the field. This field dependence is different from what is expected in the London model of a type-2 superconductor, where the magnetization should decrease logarithmically with the field for $H_{c1} \ll H \ll H_{c2}$. Recent theoretical calculations taking thermal fluctuations and topological excitations in the high- T_c superconductors explicitly into account² provide the explanation for the anomalous field dependence of the magnetization:

In the strongly anisotropic limit considered in Ref. 2 fluctuation contributions to the reversible magnetization at T_{c0} should exhibit the scaling form $M_{\text{fl}} = F(H/H_{\text{cr}})$ with $F = \text{const}$ for $H \ll H_{\text{cr}}$ and $F \sim \ln(H)$ for $H \gg H_{\text{cr}}$. H_{cr} denotes a crossover field

$$H_{\text{cr}} = (\phi_0 / \pi \gamma^2 s^2) \ln[s \gamma / 4 \xi_{ab} \sqrt{\ln(\gamma s / \xi_{ab})}] \quad (1)$$

(ϕ_0 being the flux quantum, s the layer distance, γ the anisotropy parameter, and ξ_{ab} the in-plane coherence length).

As shown in the inset of Fig. 4 we find the corresponding crossover behavior with a broad crossover field range below 10 Oe. Estimating $H_{\text{cr}} \approx 7$ Oe we derive $\gamma \approx 10^3$, i.e., a value about one order of magnitude larger than in Bi(2212).

In Fig. 5 we have plotted the imaginary part of the ac susceptibility χ'' measured at 274 Hz with a 80 mOe amplitude of the driving field by a mutual inductance technique. The ac field and the superimposed dc field were directed along the c axis of the crystal. For the definition of the irre-

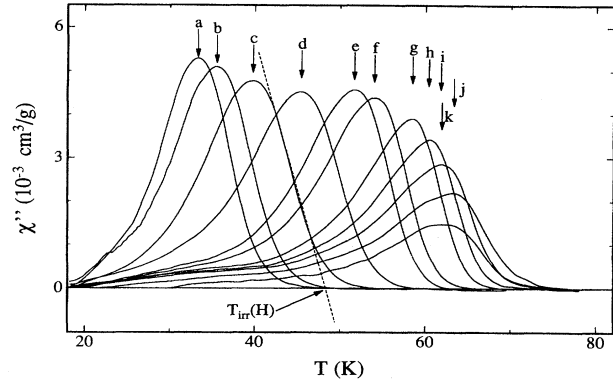


FIG. 5. Imaginary part of the ac susceptibility for different superimposed dc fields. The letters denote the dc field (a : 5400 Oe, b : 3600 Oe, c : 1800 Oe, d : 720 Oe, e : 270 Oe, f : 180 Oe, g : 72 Oe, h : 36 Oe, i : 18 Oe, j : 7.4 Oe, k : 0.2 Oe). The extrapolation procedure for the determination of $T_{\text{irr}}(H)$ is shown for curve c as an example.

versibility line we take the extrapolated onset of $\chi''(T)$, as shown in Fig. 5 for one example. With this definition any dependence of the irreversibility line from the amplitude of the driving field can be neglected. In Fig. 6 we show the irreversibility line $T_{\text{irr}}(H)$ thus determined in direct comparison with that of the Bi(2212) crystal obtained by an identical procedure. The irreversibility line of Bi(4413) is strongly shifted towards lower fields compared to Bi(2212) and exhibits a remarkable additional feature: It develops a maximum for an applied field of 2 Oe well below T_{c0} and bends backwards for lower fields. A corresponding behavior is also seen in the dc magnetization measurements of Fig. 4 below an applied field of 3 Oe.

This reentrance of the irreversibility line has been predicted theoretically within the framework of 3D vortex lattice melting theory,¹⁵ but to our knowledge has not yet been observed experimentally. The reentrance of the irreversibility line is caused by the weakening of the stiffness constants of

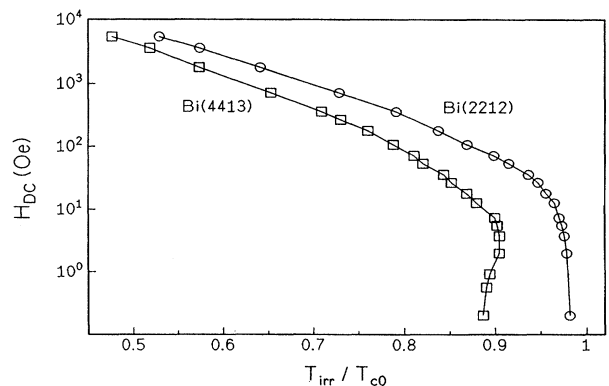


FIG. 6. Magnetic irreversibility fields versus reduced irreversibility temperature for Bi(4413) and Bi(2212). T_{c0} denotes the mean-field transition temperature.

the flux lattice in the limit of the vortex line distance $a \gg \lambda_{ab}$. Thus the result is in full agreement with the collective theory of vortex lattice melting for the high- T_c superconductors.^{1,15}

In summary, in this paper we have introduced the high- T_c phase Bi(4413) which, as expected for the large separa-

tion of the superconducting CuO_2 layers, exhibits phenomena characteristic for superconductors close to the 2D limit. In this new crystallographic phase the vortex liquid state persists down to lowest magnetic fields and for a much broader range below T_{c0} than observed for any other high- T_c phase before.

¹D. S. Fisher *et al.*, Phys. Rev. B **43**, 130 (1991).

²L. N. Bulaevskii *et al.*, Phys. Rev. Lett. **68**, 3773 (1992).

³G. Blatter *et al.*, Phys. Rev. B **48**, 10 448 (1993); P. Minnhagen and P. Olsson, Phys. Scr. **T42**, 29 (1992).

⁴J. M. Kosterlitz and D. J. Thouless, J. Phys. C **6**, 1181 (1973); J. P. Rodriguez, Phys. Rev. B **49**, 9831 (1994).

⁵S. Martin *et al.*, Phys. Rev. Lett. **62**, 677 (1989); D. A. Brawner *et al.*, *ibid.* **71**, 785 (1993); A. Schilling *et al.*, *ibid.* **71**, 1899 (1993).

⁶S. L. Lee *et al.*, Phys. Rev. Lett. **71**, 3862 (1993).

⁷D. E. Farrell *et al.*, Phys. Rev. Lett. **63**, 782 (1989).

⁸B. vom Hedt, W. LiBeck, K. Westerholt, and H. Bach, Phys. Rev. B **49**, 9898 (1994).

⁹O. Bonfigt, H. Somnitz, K. Westerholt, and H. Bach, J. Cryst. Growth **128**, 725 (1993).

¹⁰A. A. Levin *et al.*, Phys. Solid State **36**, 747 (1994) discusses a structure very similar to ours, but the authors assumed the space group *Pbmm*.

¹¹S. Vadlamannati *et al.*, Phys. Rev. B **44**, 7094 (1991).

¹²L. G. Aslamasov and A. I. Larkin, Phys. Lett. **26A**, 238 (1968).

¹³B. I. Halperin and D. R. Nelson, J. Low Temp. Phys. **36**, 599 (1979).

¹⁴R. Kubiak, K. Westerholt, and H. Bach, Physica C **166**, 523 (1990).

¹⁵D. R. Nelson, Phys. Rev. Lett. **60**, 1973 (1988).

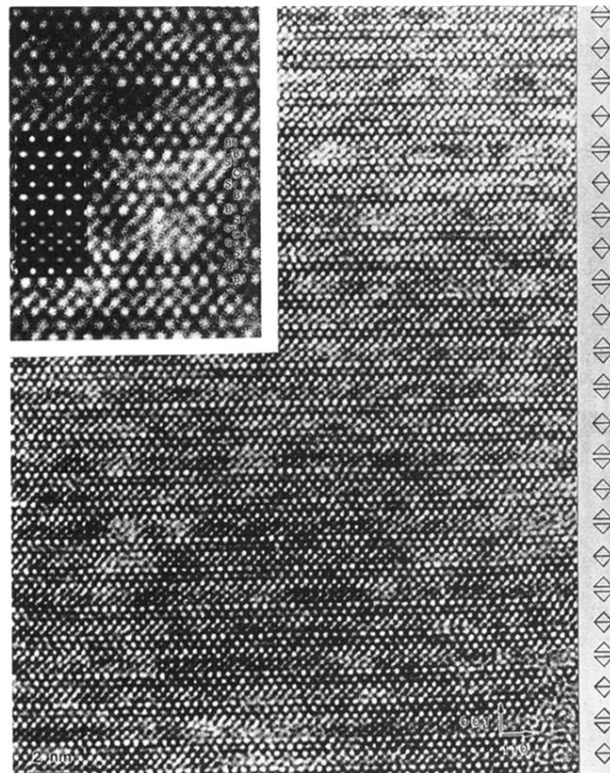


FIG. 2. HRTEM projection of Bi(4413) along the [110] direction. The inset shows an expanded view of the unit cell block compared to the image from a computer simulation. The symbols on the right margin denote the position of the CuO_2 layers.